Bioprocess Modelling

A Pharmacokinetic Model for the Metabolism of Ethanol and Acetaldehyde in Human Beings

Dragana Ristanovic, draganar@ethz.ch
George Tancev, gtancev@ethz.ch

Zurich, August 12, 2016

Contents

1. Introduction

1.1. Consumption and risks of ethanol

The oldest receipts for alcoholic (or ethanol containing) beverages, in this case for what we call beer nowadays, date back to at least the fifth millennium BC [3]. Since that time, many more developments such as wine and whiskey were made, and they became a part of the human society. The worldwide consumption in 2010 was equal to 6.2 litres of pure alcohol consumed per person aged 15 years or older, which translates into 13.5 grams of pure alcohol per day. A quarter of this consumption (24.8 %) was unrecorded, i.e., home-made alcohol, illegally produced or sold outside normal government controls. Of total recorded alcohol consumed worldwide, 50.1 % was consumed in the form of spirits [5]. The risks that come from drinking beer, wine, whiskey, and so on are not to be sneezed at. In 2012, about 3.3 million deaths, or 5.9 % of all global deaths, were attributable to alcohol consumption [5]. On one site, there are direct causes of death, as ethanol is metabolised to acetaldehyde, which is toxic. It causes cardiac arrhythmias, nausea, anxiety, and facial flushing. On the other site, there are indirect deaths, e.g. car accidents, as a consequence of the nausea. Therefore, it is important to track the amounts of ethanol and acetaldehyde in the body [2].

1.2. Problem definition

Despite the social graces of alcoholic beverages, one has to be performance-capable after a night of drinking. There are different questions that come up; how much can someone afford to drink until midnight in order not to have a hangover the next morning? Or when does one have to stop at the latest? A mathematical model could answer such questions, but a definition and feasible quantification of "performance-capable" is needed first.
However, there are several issues in gathering experimental data. It is quite challenging to determine the concentration of free acetaldehyde in the blood on the basis of either breath or blood analysis methods. Artefactual formation of acetaldehyde hinders precise blood analysis, and production by microorganisms in the throat inhibits the determination from breath assays. In addition, a lot of the acetaldehyde present in the blood is bound to plasma proteins and haemoglobin. Only the free acetaldehyde crosses the alveolarcapillary membranes of the lungs. Therefore, breath tests give only an approximation of free acetaldehyde in the blood [2].
From the numerical perspective, such a model would consist of a set of differential equations, which might lead to stiffness. Thus, the parameter estimation itself might be computationally expensive.

1.3. Aim of the project

The aim of this work was to present a pharmacokinetic model that describes the ethanol metabolism in human beings and to perform a parameter estimation based on in silico generated data. Furthermore, a model analysis should provide information about the quality of the estimated parameters. Model improvement was not part of the aim of this project as all data were generated from the model itself.

2. Methods

2.1. Model construction: equations and assumptions

Due to the reasons mentioned above, a time-resolved prediction of the ethanol and acetaldehyde concentrations in the human body would be desired. One possibility is a pharmacokinetic model in which the body is separated into different compartments. In principle, the model could be mass and/or age dependent, but this would lead to a much higher complexity, because the mass and age dependence of fluids, organs, enzymes, and so on is not straightforward. Therefore, the model is designed for a middle-aged male person of 70 kg. The body is separated into five compartments, namely stomach, gastrointestinal tract, liver, central fluid, as well as muscle and fat. Except for the liver, all of them are continuously stirred tanks (CST). The liver is being modelled as a cascade of N continuously stirred tank reactors (CSTRs), in order to approximate a plug-flow reactor (PFR) [2]. N was set to 10, because further addition of units did not change the behaviour significantly. A scheme of the system is shown in Fig. 1.

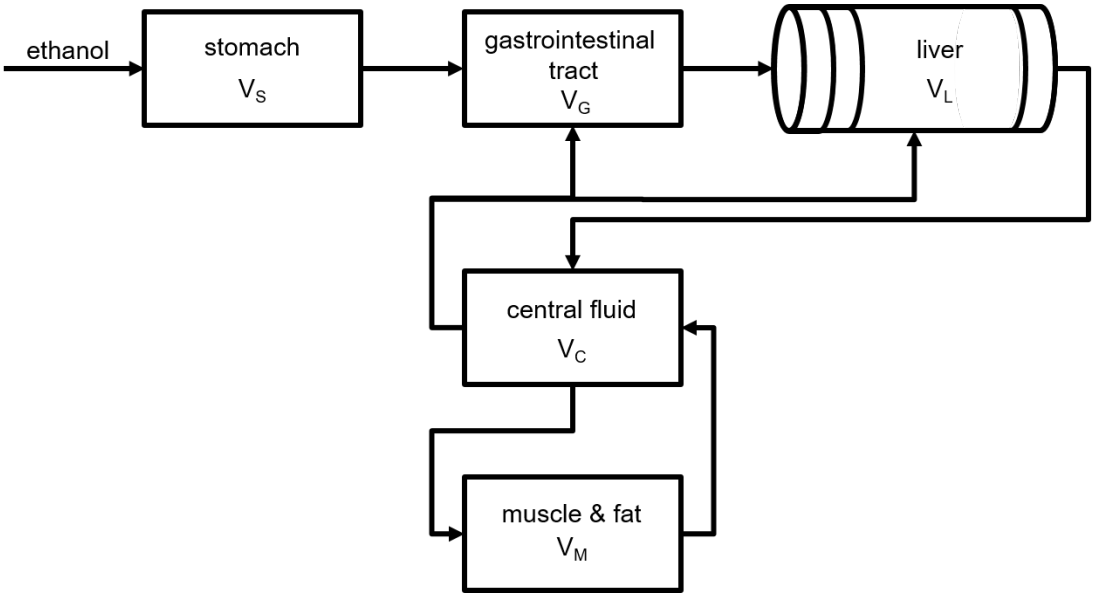

Figure 1: Schematic drawing of the model topology [2].

The model is dynamic and consists of a set of ordinary differential equations (ODEs) which are mass balances between the different compartments [2]. The rate law of ethanol oxidation was based on the alcohol dehydrogenase (ADH) reaction pathway, as this is the largest contributor to ethanol oxidation. Consequently, the transformation of ethanol to acetaldehyde occurs only in the liver. It is reversible and described by a Michaelis-Menten mechanism. Nicotinamide adenine dinucleotide (NADH) is the co-substrate and serves as an energy source for the reaction. It is assumed that the concentration of NAD^+ (oxidised form of NADH) reaches its rate-limiting state right after ingestion and then remains constant. This means that ethanol elimination is approximately of zero order. Further it is assumed that the net rate of formation of the substrate-enzyme complexes is zero, which means that pseudo steady state approximation can be used. The only difference in the derivation of the rate law equations for acetaldehyde oxidation to acetic acid is the assumption of an irreversible reaction. The largest contributor to acetaldehyde oxidation is the mitochondrial class 2 aldehyde dehydrogenase (ALDH2), which accounts for more than 99% of oxidised acetaldehyde in the human body. The reaction pathway is shown in Fig. 2. The reactions are shown in the appendix.

2.1.1. Stomach

$$\frac{dV_{\mathrm{s}}}{dt} = -k_{\mathrm{s}}(V_{\mathrm{s}}) \tag{1}$$

$$k_{\mathrm{s}} = \frac{k_{\mathrm{s,max}}}{1 + a(\frac{D}{1000})^2} \tag{2}$$

Ethanol is absorbed primarily by the duodenum and less by the mucosa in the stomach [4]. Therefore, ethanol entering the duodenum is virtually instantaneously transferred to the gastrointestinal tract. Hence, ethanol absorption by the duodenum can be approximated by the rate at which ethanol is emptied. This change of volume of alcoholic beverage in the stomach V_{s}, can be described by a first order relation (see Eq. 1), where the stomach-emptying rate constant k_{s} is dependent on the initial dose of ethanol in the system D ($D = C_{\mathrm{Al}}V^0_{\mathrm{Al}}$), a maximum emptying rate constant $k_{\mathrm{s,max}}$, and an empirical parameter a.

2.1.2. Gastrointestinal tract

$$V_{\mathrm{G}}\frac{dC_{\mathrm{G,Al}}}{dt} = \frac{2}{3}Q_{\mathrm{L}}(C_{\mathrm{C,Al}} - C_{\mathrm{G,Al}}) + k_{\mathrm{s}}(V_{\mathrm{s}})(C_{\mathrm{S,Al}}) \tag{3}$$

$$V_{\mathrm{G}}\frac{dC_{\mathrm{G,Ac}}}{dt} = \frac{2}{3}Q_{\mathrm{L}}(C_{\mathrm{C,Ac}} - C_{\mathrm{G,Ac}}) \tag{4}$$

The stomach content is emptied and transferred to the gastrointestinal system, which has a tissue water volume of V_{G}. Considering the model topology presented in Fig. 1, the blood flow rate through the gastrointestinal system is equal to the blood flow rate entering the liver by means of the hepatic portal vein. This flow rate is approximately two thirds of the total blood flow rate to the liver ($\frac{2}{3}Q_{\mathrm{L}}$). The mass balances for ethanol and acetaldehyde in the gastrointestinal tract are given by Eq. 3 and 4. In these equations, V_{G} is the gastrointestinal system tissue water volume, Q_{L} is the total liver blood flow rate, $C_{\mathrm{G,Al}}$ and $C_{\mathrm{C,Al}}$ are the gastrointestinal and central compartment ethanol concentrations, respectively, and $C_{\mathrm{G,Ac}}$ and $C_{\mathrm{C,Ac}}$ are the corresponding concentrations of acetaldehyde. Finally, V_{s} and k_{s} are the volume of ethanol in the stomach compartment and the stomach-emptying rate, introduced in the previous section, and $C_{\mathrm{S,Al}}$ is the stomach compartment ethanol concentration, which depends on type of alcoholic beverage.

2.1.3. Liver

$$\Delta V_{\mathrm{L}}\frac{dC_{\mathrm{N,Al}}}{dt} = Q_{\mathrm{L}}(C_{\mathrm{N\text{-}1,Al}} - C_{\mathrm{N,Al}}) + r_{\mathrm{Al}}(C_{\mathrm{N,Al}}, C_{\mathrm{N,Ac}})\Delta V_{\mathrm{L}} \tag{5}$$

$$\Delta V_{\mathrm{L}}\frac{dC_{\mathrm{N,Ac}}}{dt} = Q_{\mathrm{L}}(C_{\mathrm{N\text{-}1,Ac}} - C_{\mathrm{N,Ac}}) - r_{\mathrm{Al}}(C_{\mathrm{N,Al}}, C_{\mathrm{N,Ac}})\Delta V_{\mathrm{L}} + r_{\mathrm{Ac}}(C_{\mathrm{N,Ac}})\Delta V_{\mathrm{L}} \tag{6}$$

$$-r_{\mathrm{Al}} = \frac{V_{\mathrm{max,\ ADH}}C_{\mathrm{Al}} - V_{\mathrm{rev,\ ADH}}C_{\mathrm{Ac}}}{K_{\mathrm{m,ADH}} + C_{\mathrm{Al}} + K_{\mathrm{rev,ADH}}C_{\mathrm{Ac}}} \tag{7}$$

$$-r_{\mathrm{Ac}} = \frac{V_{\mathrm{max,ALDH}}C_{\mathrm{Ac}}}{K_{\mathrm{m,ALDH}} + C_{\mathrm{Ac}}} \tag{8}$$

After exiting the gastrointestinal tract, the ethanol in the blood flows to the liver through the hepatic portal vein. In addition, the liver receives blood from the hepatic artery, which supplies the other one third of the total liver blood flow. Ethanol and acetaldehyde are oxidised only within the liver to acetaldehyde and acetic acid, respectively. Because of the complexity of the forward and reverse reactions in the system, an unsteady philologically based perfusion liver model is used (series of CSTRs). The mass balances for ethanol and acetaldehyde in the

compartment $i \in [1,N]$ are given in Eq. 5 and 6. In these equations, ΔV_L represents the water tissue volume of one "slice" of the liver ($\Delta V_L = V_L/N$), $-r_{Al}$ and $-r_{Ac}$ represent the rate of reaction of ethanol and acetaldehyde, respectively. Both components exit the liver by means of the hepatic vein into the central compartment with concentrations $C_{N,Al}$ and $C_{N,Ac}$.

2.1.4. Central fluid

$$V_C \frac{dC_{C,Al}}{dt} = -Q_L(C_{C,Al} - C_{M,Al}) - Q_M(C_{C,Al} - C_{M,Al}) \quad (9)$$

$$V_C \frac{dC_{C,Ac}}{dt} = -Q_L(C_{C,Ac} - C_{M,Al}) - Q_M(C_{C,Ac} - C_{M,Al}) \quad (10)$$

The total tissue water volume of the central compartment V_C is the sum of all tissue water volumes of its components: blood, bone, brain, kidneys, lungs, skin, heart, and spleen (organs with a perfusion rate greater than 0.08 mL (min mL)$^{-1}$. This compartment is modelled as a well mixed tank without reaction. The mass balances for ethanol and acetaldehyde are given in Eq. 9 and 10. Q_L is the total liver blood flow rate and Q_M is the blood flow rate to the muscle & fat compartment. $C_{M,Al}$ and $C_{C,Al}$ are the ethanol concentrations in the muscle and central compartment, and $C_{M,Ac}$ and $C_{C,Ac}$ are the corresponding concentrations of acetaldehyde. $C_{L,Al}$ and $C_{L,Ac}$ are the ethanol and acetaldehyde concentrations in the liver compartment.

2.1.5. Muscle & fat

$$V_M \frac{dC_{M,Al}}{dt} = Q_M(C_{C,Al} - C_{M,Al}) \quad (11)$$

$$V_M \frac{dC_{M,Ac}}{dt} = Q_M(C_{C,Ac} - C_{M,Ac}) \quad (12)$$

This compartment is comprised of all tissues with a perfusion rate less than 0.08 mL (min mL)$^{-1}$. The average perfusion rate of this compartment is significantly lower than the one of other compartments, which is important for the kinetics of the ethanol distribution and elimination. Mass balances for ethanol and acetaldehyde are given by Eq. 11 and 12. V_M is the water tissue volume of the muscle and fat compartment, Q_M. $C_{M,Al}$ and $C_{C,Al}$ are the concentrations of ethanol in the muscle and central compartment, and $C_{M,Ac}$ and $C_{C,Ac}$ are the corresponding concentrations of acetaldehyde.

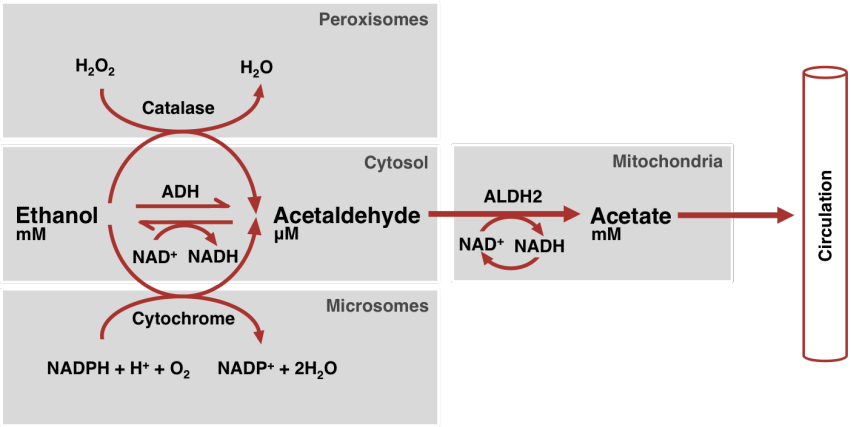

Figure 2: Detailed representation of ethanol metabolism in the human body. In the mathematical model, only the metabolism based on the alcohol dehydrogenase (ADH) pathway is considered as it is the largest contributor to ethanol oxidation [2].

2.2. Data

Tab. 1 shows the known parameters/data of the compartments.

Table 1: Overview of compartments and their respective volumes and flowrates [1].

compartment	**tissue(s)**	**data**	
stomach	stomach	C_{Al}	1625 mM
		$\mathrm{V}_{\mathrm{s}}^{0}$	0.15 L
gastrointestinal tract	stomach/intestine	V_{G}	2.4 L
		Q_{L}	1.35 L min^{-1}
liver	liver	N	10
		ΔV_{L}	0.11 L
		Q_{L}	1.35 L min^{-1}
central fluid	lungs	V_{C}	11.56 L
	kidneys	Q_{L}	1.35 L min^{-1}
	brain		
	heart		
	skin		
	bone		
	blood		
muscle	muscle	V_{M}	25.8 L
	fat	Q_{M}	1.50 L min^{-1}

2.3. Parameter estimation

The unknown parameters in the model, that have to be estimated, are

$k_{\mathrm{s,max}}$ the maximum stomach emptying constant

a an empirical parameter

$V_{\mathrm{max,ADH}}$ maximum enzymatic oxidation rate of ethanol

$V_{\mathrm{rev,ADH}}$ maximum rate of the reverse reaction of acetaldehyde to ethanol

$K_{\mathrm{m,ADH}}$ reaction constant for the rate law

$K_{\mathrm{rev,ADH}}$ reaction constant for the rate law

$V_{\mathrm{max,ALDH}}$ maximum enzymatic oxidation rate of acethaldehyde

$K_{\mathrm{m,ALDH}}$ reaction constant for the rate law

The coefficient of variation (c_{v}) of the output variables was provided. From this, the covariance matrix (V_{ϵ}) could be computed.

$$c_{\mathrm{v}} = \frac{\sigma}{\mu} = 0.05 \tag{13}$$

$$V_{\epsilon} = \mathrm{diag}\left(\sigma^2\right) \tag{14}$$

The parameters were estimated by a maximum likelihood estimation (MLE) on MATLAB, using an ODE solver for stiff equations (ode15s). The objective function is given by Equation 2.13.

$$\Phi_{\mathrm{ML}} = (y_{\mathrm{m}} - y)^T V_{\epsilon} (y_{\mathrm{m}} - y) \tag{15}$$

The bounds in the parameter search space were set as $p_{\mathrm{i}} \in [0{,}100]$. The initial value, p_{initial}, was taken from an OLS estimation which was performed before the MLE.

3. Results and Discussion

3.1. Parameter estimation

The parameters from the MLE are listed in Tab. 2.

Table 2: Estimated parameters of the ML.

$k_{s,max}$ / min^{-1}	a / $mmol^{-2}$	$V_{max,ADH}$ / $mM\,min^{-1}$	$V_{rev,ADH}$ / $mM\,min^{-1}$	$K_{m,ADH}$ / mM	$K_{rev,ADH}$ / mM	$V_{max,ALDH}$ / $mM\,min^{-1}$	$K_{m,ALDH}$ / mM
0.468	71.811	1.810	62.631	0.388	80.388	2.796	0.002

In Fig. 3–7, the experimental data are compared with the model results. From the figures, the fitting looks good and the residual plots indicate no trend, meaning that the error between model prediction and experimental data is random. In order to evaluate the quality of the parameter estimation, an identifiability analysis is also necessary.

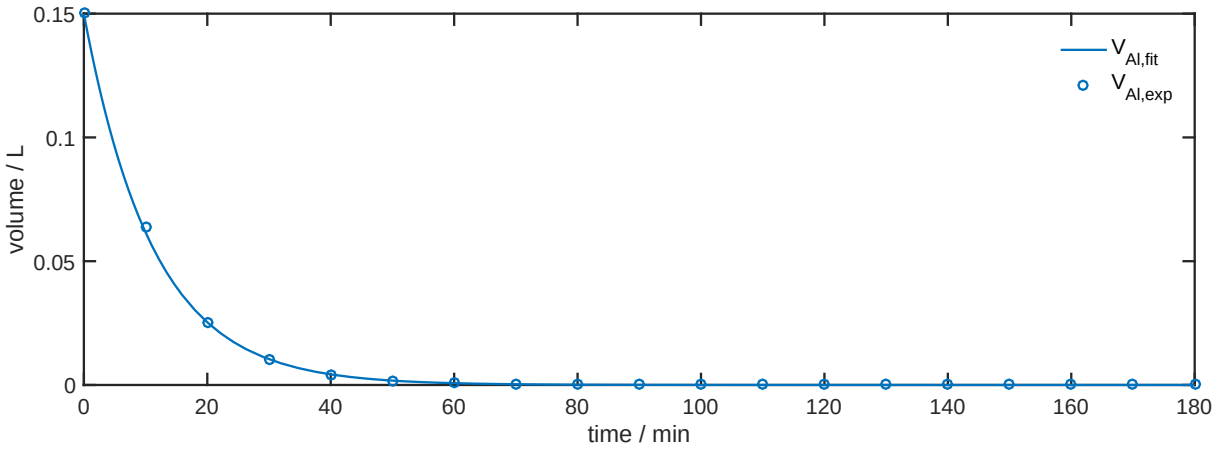

Figure 3: Volume profile in the stomach.

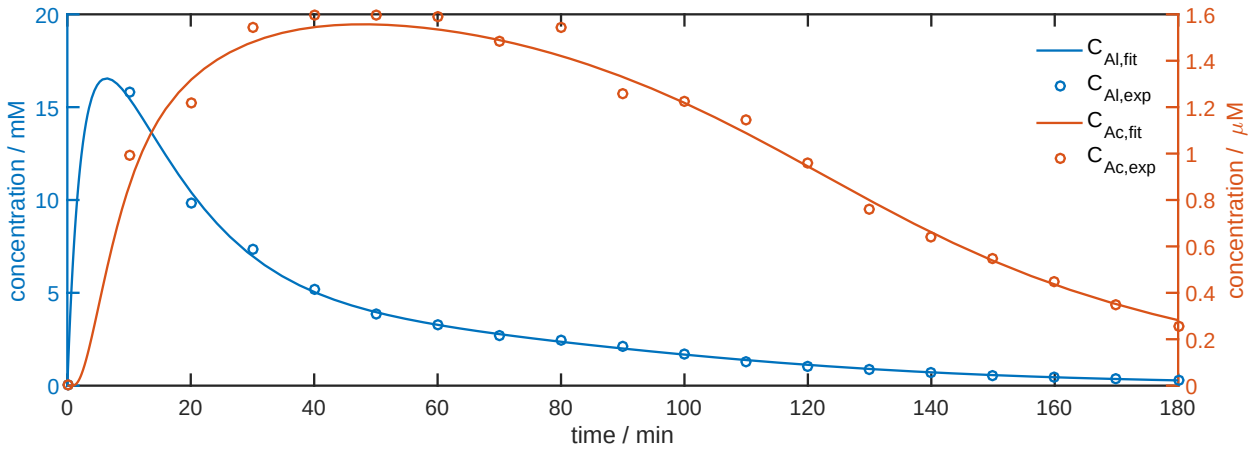

Figure 4: Concentration profile in the gastricular tract.

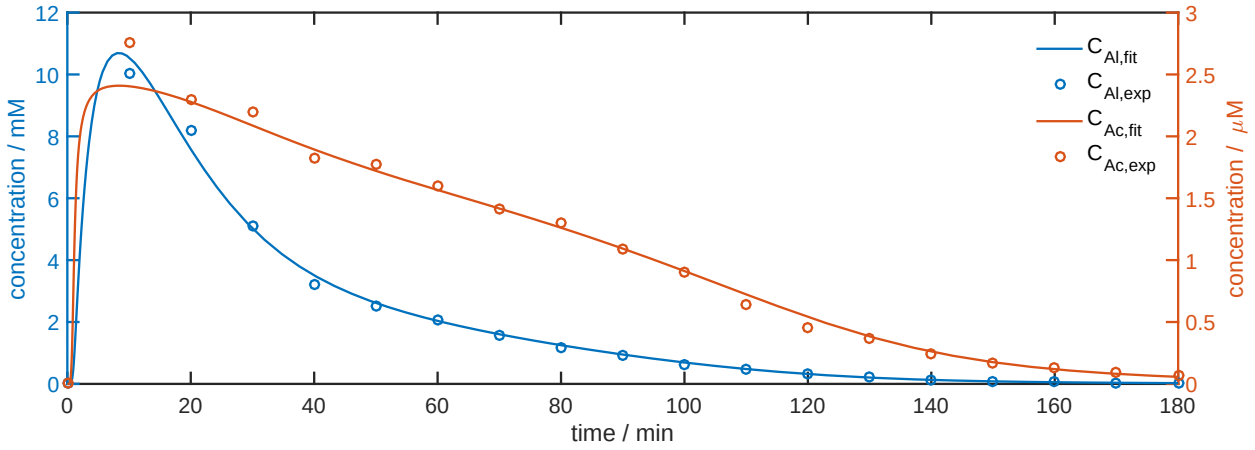

Figure 5: Concentration profile in the last compartment of the liver.

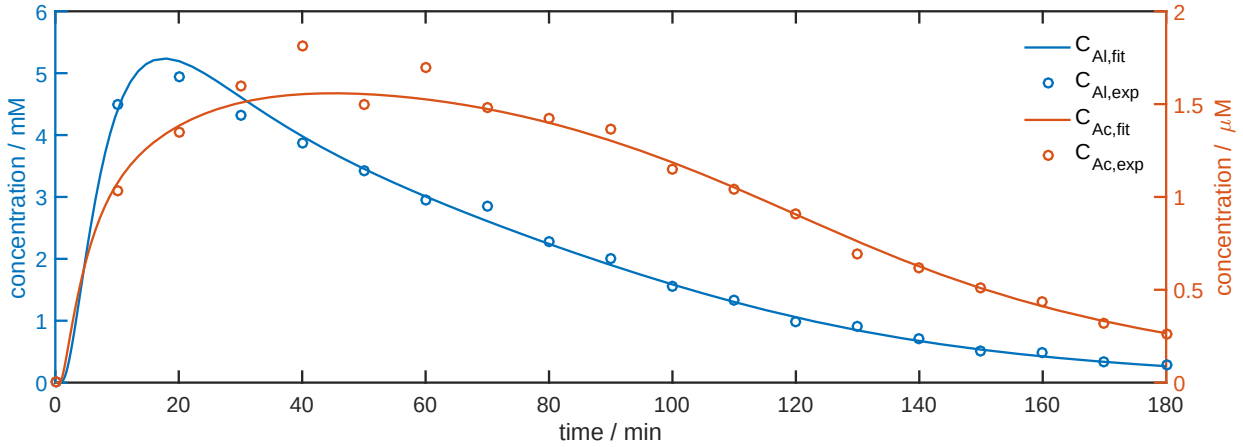

Figure 6: Concentration profile in the central fluid.

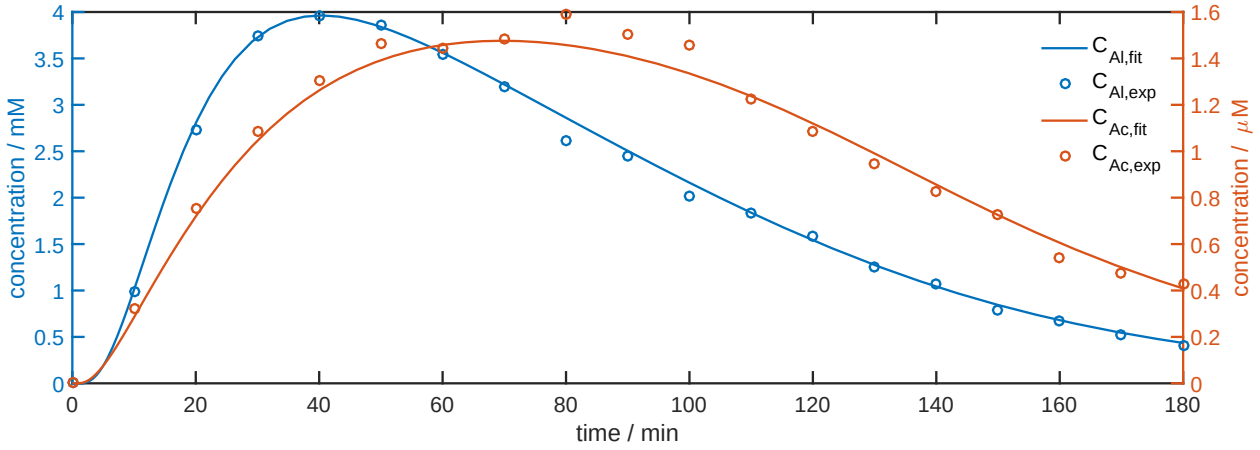

Figure 7: Concentration profile in muscle & fat.

3.2. Identifiability analysis

3.2.1. Stuctural identifiability

The rank of the sensitivity matrix ($\text{rank}(S) = 7$) is lower than the number of parameters ($n_\text{p} = 8$). Therefore, one parameter is not a priori identifiable, but the rank assessment does not state which subset of parameters can be estimated. There are different possibilities to identify this (or those) parameters. For a small amount of parameters, the existence of a perfect correlation between parameters can be proved if the sum of the sensitivity coefficients for two parameters on the same response variable is zero at all times. Thus, these parameters cannot be estimated simultaneously [6]. In this case, k_s is a function of $k_\text{s,max}$ and a. Hence, there are many possible combinations of them that provide a good fit for the volume in the stomach.
Other possibilities are the algorithm proposed by Yao et. al or a single value decomposition [6].

3.2.2. Practical identifiability

By determining the sensitivities by the direct method, the variance of the parameters and the 97.5 % confidence intervals were estimated (Tab. 3) by computing the Fisher information matrix (FIM). The lower bound for the variance of the parameters (V_p) is given by the inverse of the FIM. Higher values in the FIM (higher sensitivities or lower uncertainty in the data) will increase the precision of the estimators.

	p_i				
$k_\text{s,max}$	-74302.986	$\leq$	0.468	$\leq$	74303.922
a	-14087052.441	$\leq$	71.811	$\leq$	14087196.063
$V_\text{max,ADH}$	1.787	$\leq$	1.810	$\leq$	1.832
$V_\text{rev,ADH}$	-8285.114	$\leq$	62.631	$\leq$	8410.376
$K_\text{m,ADH}$	-4.238	$\leq$	0.388	$\leq$	5.013
$K_\text{rev,ADH}$	-2898.696	$\leq$	80.388	$\leq$	3059.472
$V_\text{max,ALDH}$	2.733	$\leq$	2.796	$\leq$	2.858
$K_\text{m,ALDH}$	0.002	$\leq$	0.002	$\leq$	0.002

Table 3: Estimated parameters of the ML and their respective confidence intervals.

Hence, five of eight parameters are not practically identifiable, as the sign between lower and upper bound of the confidence intervals changes. The reason for this is the (large) correlation of some of the parameters, which can be seen in V_p (the inverse of FIM) in Tab. 4. Especially the variances and covariances of $k_\text{s,max}$ and a are outstanding. But $V_\text{rev,ADH}$, $K_\text{m,ADH}$, and $K_\text{rev,ADH}$ have large (co)variances, too.

$V_\text{p} \geqslant$

	$k_\text{s,max}$	a	$V_\text{max,ADH}$	$V_\text{rev,ADH}$	$K_\text{m,ADH}$	$K_\text{rev,ADH}$	$V_\text{max,ALDH}$	$K_\text{m,ALDH}$
$k_\text{s,max}$	$5.4 \cdot 10^{8}$	$1.0 \cdot 10^{11}$	$2.6 \cdot 10^{-3}$	$2.8 \cdot 10^{1}$	$-1.5 \cdot 10^{-2}$	-9.7	$1.1 \cdot 10^{-2}$	$9.0 \cdot 10^{-6}$
a	$1.0 \cdot 10^{11}$	$2.0 \cdot 10^{13}$	$5.0 \cdot 10^{-2}$	$5.6 \cdot 10^{3}$	-2.9	$-1.9 \cdot 10^{3}$	2.1	$1.7 \cdot 10^{-3}$
$V_\text{max,ADH}$	$2.6 \cdot 10^{-3}$	$5.0 \cdot 10^{-2}$	$1.3 \cdot 10^{-4}$	3.0	$-1.7 \cdot 10^{-3}$	$-9.5 \cdot 10^{-1}$	$1.9 \cdot 10^{-4}$	$1.9 \cdot 10^{-9}$
$V_\text{rev,ADH}$	$2.8 \cdot 10^{1}$	$5.6 \cdot 10^{3}$	3.0	$1.8 \cdot 10^{7}$	$-1.0 \cdot 10^{4}$	$-6.4 \cdot 10^{6}$	$1.3 \cdot 10^{1}$	$1.7 \cdot 10^{-2}$
$K_\text{m,ADH}$	$-1.5 \cdot 10^{-2}$	-2.9	$-1.7 \cdot 10^{-3}$	$-1.0 \cdot 10^{4}$	5.5	$3.6 \cdot 10^{3}$	$-7.5 \cdot 10^{-3}$	$-9.2 \cdot 10^{-6}$
$K_\text{rev,ADH}$	-9.7	$-1.9 \cdot 10^{3}$	$-9.5 \cdot 10^{-1}$	$-6.4 \cdot 10^{6}$	$3.6 \cdot 10^{3}$	$2.3 \cdot 10^{6}$	-4.7	$-5.9 \cdot 10^{-3}$
$V_\text{max,ALDH}$	$1.1 \cdot 10^{-2}$	2.1	$1.9 \cdot 10^{-4}$	$1.3 \cdot 10^{1}$	$-7.5 \cdot 10^{-3}$	-4.7	$1.0 \cdot 10^{-3}$	$1.0 \cdot 10^{-6}$
$K_\text{m,ALDH}$	$9.0 \cdot 10^{-6}$	$1.7 \cdot 10^{-3}$	$1.9 \cdot 10^{-9}$	$1.7 \cdot 10^{-2}$	$-9.2 \cdot 10^{-6}$	$-5.9 \cdot 10^{-3}$	$1.0 \cdot 10^{-6}$	$1.1 \cdot 10^{-9}$

Table 4: Covariance matrix of the estimated parameters.

3.3. Design of experiments

In order to obtain smaller confidence intervals, a design of experiments was performed. The initial volume of wine in the stomach was varied and the trace of the Fisher information matrix was computed (T-optimal design). A higher value of the trace means that the inverse of the FIM (and the respective confidence intervals) become smaller.

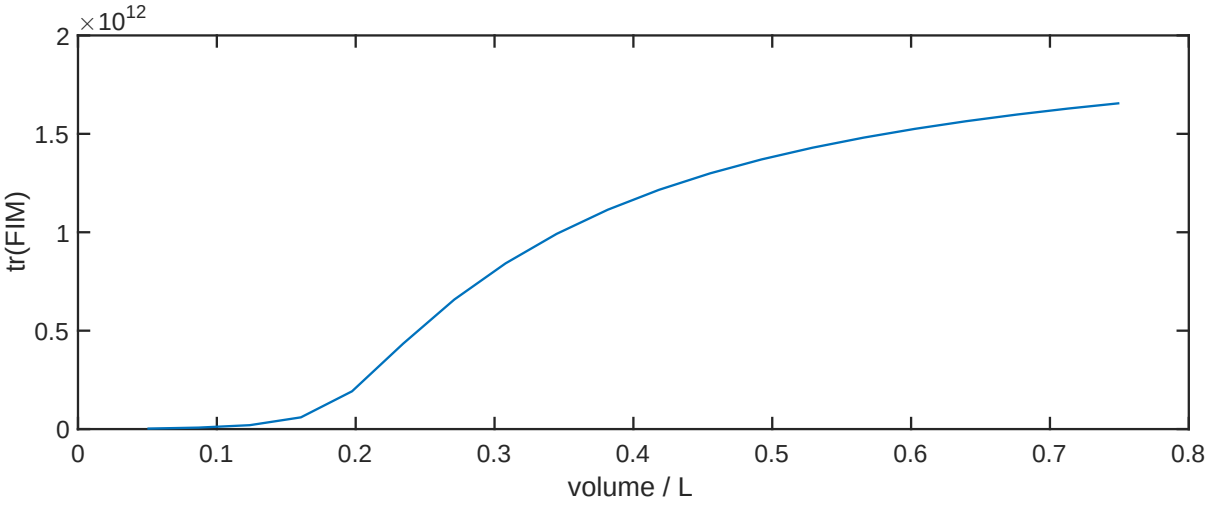

Figure 8: Initial volume of wine in the stomach vs. trace of FIM.

Fig. 8 shows that a higher initial volume of wine should result in smaller confidence intervals. Nevertheless, it does not make any sense to increase this value infinitely, as a person would not drink that much in such a short time.

4. Summary

Summing up, a pharmacokinetic model for the ethanol metabolism in human beings was developed. It consists of five compartments, namely stomach, gastrointestinal tract, liver, central fluid, and muscle & fat. Most of the compartments were modelled as stirred tanks. Only the liver was described by an unsteady physiologically based perfusion model (cascade of CSTRs). It was assumed that the oxidation of ethanol to acetaldehyde was reversible and that it is mainly metabolised by ADH (main contributor). Acetaldehyde was assumed to react irreversibly to acetic acid, catalysed by ALDH2.
Experimental data was generated in silico using the proposed model, what makes later model invalidation redundant. The parameter estimation of the model converged, but many parameters were not identifiable, either structural, practical, or both. This information was obtained by performing a sensitivity analysis. The reason for the non-identifiability was a strong correlation within two subsets of parameters.
Finally, to overcome these issues, a design of experiments (T-optimal) was carried out by varying the initial amount of alcoholic beverage in order to find a better experimental condition. The T-optimal design minimises the dimension of the enclosing box around the joint confidence region.
The model analysis can be arbitrarily extened. For exemple, the influence of certain substances can be examinated by the Green's function method, if ADH, ALDH2, or other chemicals were injected at time $\tau \geqslant t$. This could help modelling treatments for alcohol intoxications.
However, the initially posed question is not answerable, as no reference value of acetaldehyde in the blood could be found. The authors would be willing to provide alcoholic beverages to volunteers in order to gather more data.

A. Degradation mechanism

The corresponding reaction equations for the degradation mechanism are listed below.

A.1. Ethanol

$$\mathrm{CH_3CH_2OH} + \mathrm{ADH} \underset{NADH}{\overset{NAD^+}{\rightleftharpoons}} \mathrm{CH_3CH_2OH{\bullet}ADH}$$

$$\mathrm{CH_3CH_2OH{\bullet}ADH} \underset{NADH}{\overset{NAD^+}{\rightleftharpoons}} \mathrm{CH_3CHO{\bullet}ADH} + \mathrm{H_2O}$$

$$\mathrm{CH_3CHO{\bullet}ADH} \rightleftharpoons \mathrm{CH_3CHO} + \mathrm{ADH}$$

A.2. Acetaldehyde

$$\mathrm{CH_3CHO} + \mathrm{ALDH2} \underset{NADH}{\overset{NAD^+}{\rightleftharpoons}} \mathrm{CH_3CHO{\bullet}ALDH2}$$

$$\mathrm{H_2O} + \mathrm{CH_3CHO{\bullet}ALDH2} \underset{NADH}{\overset{NAD^+}{\rightleftharpoons}} \mathrm{CH_3COOH{\bullet}ALDH2}$$

$$\mathrm{CH_3COOH{\bullet}ALDH2} \longrightarrow \mathrm{CH_3COOH} + \mathrm{ALDH2}$$

References

[1] M. Rowland, T. N. Tozer, and R. Rowland. Clinical Pharmacokinetics: Concepts and Applications. Lippincott Williams & Wilkins, 3 edition, 1995.

[2] D. M. Umulis, N. M. Gurmen, P. Singh, and H. S. Fogler. Alcohol, 35:3–12, 2005.

[3] J. Wanga, L. Liua, T. Ballc, L. Yud, Y. Lie, and F. Xing. PNAS, 113:6444–6448, 2016.

[4] P. K. Wilkinson, A. J. Sedman, E. Sakmar, D. R. Kay, and J. G. Wagner. Journal of Pharmacokinetics and Biopharmaceutics, 5:207–224, 1977.

[5] World Health Organisation (WHO). Global Status Report on Alcohol and Health, 2014.

[6] K. Z. Yao, B. M. Shaw, B. K., K. B. McAuley, and D. W. Bacon. Polymer Reaction Engineering, 11:563–588, 2003.